An ONIOM2 study on pyridine adsorption in the main channels of Li- and Na-MOR

5 AUTHORS, INCLUDING:

Yun-Bo Duan

Qingdao University

41 PUBLICATIONS **407** CITATIONS

Yong-Wang Li

Chinese Academy of Sciences

403 PUBLICATIONS **7,309** CITATIONS

An ONIOM2 study on pyridine adsorption in the main channels of Li- and Na-MOR

Shuping Yuan [a,b,*], Jianuo Wang [b], Yun-Bo Duan [a], Yong-Wang Li [b], Haijun Jiao [b,c]

[a] Institute for Computational Science and Engineering, Qingdao University, Qingdao 266071, China
[b] State Key Laboratory of Coal Conversion, Institute of Coal Chemistry, Chinese Academy of Sciences, P.O. Box 165, Taiyuan 030001, China
[c] Leibniz-Institut für Katalyse e.V. an der Universität Rostock, Albert-Einstein-Strasse 29a, 18059 Rostock, Germany

Abstract

A 24T model containing a complete two-layered 12-membered ring connected by an 8-membered side pocket was used to represent the channel of the MOR framework. On the basis of this model, the structures of the acid sites in the main channels of Li- and Na-MOR as well as their interaction with pyridine probe molecule were investigated using the ONIOM2 (QM/QM; B3LYP/6-31G(d,p):HF/3-21G) and ONIOM2 (QM/MM; B3LYP/6-31G(d,p):UFF) methods. There are two stable structures for the Li-MOR cluster; one has Li$^+$ interacting with two oxygen atoms around Al, and the other has Li$^+$ interacting with four oxygen atoms belonging to a five-membered ring. This four-fold Li$^+$ coordination is consistent with Na$^+$ in Na-MOR, and is the same as the Na$^+$ coordination in the intersection model of Na-ZSM-5. The ONIOM2 (QM/MM) method overestimates the adsorption energies of pyridine (195.0/192.8 and 170.6 kJ/mol for Li-MOR and Na-MOR, respectively), while the ONIOM2 (QM/QM) method gives reasonable results (171.6/154.7 and 131.3 kJ/mol, respectively) compared to the available experimental values (153–195 and 120 kJ/mol, respectively). The structural parameters of the adsorption complexes showed that coordination of the alkali ion to the nitrogen atom of pyridine dominates the overall interaction between the zeolite and pyridine, and the adsorption complexes were further stabilized by hydrogen bonding between the hydrogen atoms of pyridine and the lattice oxygen atoms of the zeolite framework.
© 2006 Elsevier B.V. All rights reserved.

Keywords: MOR; Pyridine; Adsorption; ONIOM; DFT

1. Introduction

Zeolites are solid acidic catalysts widely used for hydrocarbon processing in petroleum and chemical industries. Due to the specific balance of acidic and basic functions, alkali metal ion-exchanged zeolites are found to be potential catalysts in reactions such as side-chain alkylation of toluene [1], condensation reactions [2] and selective alkylation of aromatic hydrocarbons containing oxygen or nitrogen [3], or as selective sorbents in separation technologies [4]. Among various types of zeolite, mordenite (MOR) is well known for cracking of hydrocarbons, dewaxing of heavy petroleum fractions and methanol conversion to hydrocarbons, and is also commercially used in petrochemistry to catalyze aromatic hydrocarbon isomerization reactions for its appropriate acidity and pore size as well as the thermal stability [5,6].

As the first step of chemical reactions in heterogeneous catalysis, adsorption of reactant molecules to the active site of catalyst is crucial for the efficiency of catalytic reactions. In the past years, much effort has been devoted to the investigation of the adsorption properties of zeolite catalysts from both theoretical [7–15] and experimental [16–20] viewpoints. Among the theoretical studies, most of the work used small clusters to simulate the active site in zeolites [7–12]. It is shown that although small clusters can simulate zeolite reactivity, there exists a more complex relationship between reactant and zeolite catalyst. Especially, electron delocalization from acid site atoms to other zeolite framework atoms has been shown to be important in reaction [21]. Therefore, it becomes important to use larger clusters including not only the acid site but also a significant zeolite framework surrounding the acid site to represent the zeolite channel structures.

---

* Corresponding author. Tel.: +86 532 85950690; fax: +86 532 85950690.
E-mail address: spyuan@tch.qdu.edu.cn (S. Yuan).

For large clusters, high-level computations are very time-consuming or nearly impossible, while low-level calculations lower the quality of the results. One efficient way to resolve such a dilemma is the ONIOM methods [22–24], in which the system can be partitioned into two or more layers. The regions in close relationship to the catalytic reactions can be treated more accurately by high-level methods, while those regions of low importance can be treated by a less accurate method. In recent years, the ONIOM methods have been frequently used to study the adsorption of probe molecules in zeolite pores [13–15,25–29].

Different molecules can be used as probes to explore different properties of zeolites, such as pore size and acidity. NH$_3$-TPD is often used to investigate the acidity of zeolites [7,8,10], while pyridine is frequently used as a probe of zeolite acidity in IR [30], TPD [31], XPS [32] and NMR techniques [33]. In this study, there is another reason to choose pyridine as the probe molecule, since it has a dimension close to the aromatic hydrocarbon molecules, the latter being often transformed on MOR catalyst.

This work reports the adsorption of pyridine in the main channels of Li- and Na-MOR simulated by a 24T model and calculated with the ONIOM2 method. The structures of the alkali ion-exchanged MOR and their pyridine adsorption complexes are discussed, and the calculated adsorption energies are compared to the experimental results. The two different strategies of the ONIOM2 method (QM/QM and QM/MM) on this kind of calculation are also compared and discussed.

2. Computational details

2.1. Models

The coordination of the atoms in this work is taken from the structure of Na-MOR [34], which has a multiple pore-system with main channels of 12-membered rings connected by 8-membered rings (Fig. 1). The cluster model employed to
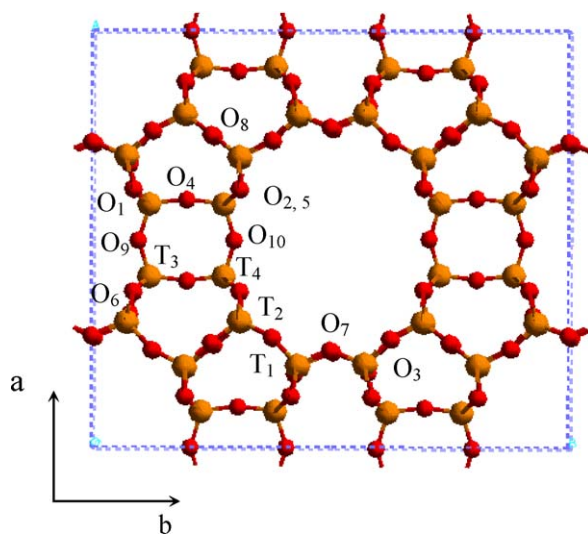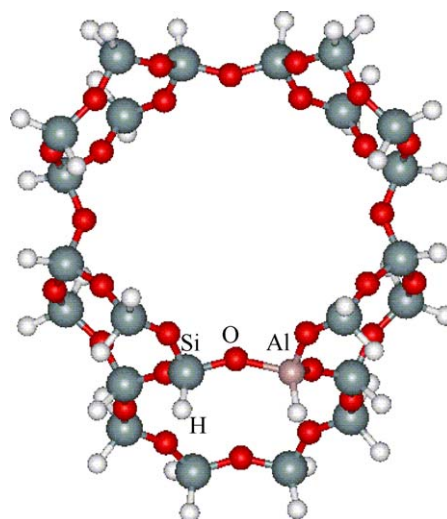

Fig. 1. Structure of mordenite unit-cell viewed down the c-axis (T$_1$, T$_2$, T$_3$, T$_4$ and O$_1$–O$_{10}$ are designated. Note that O$_2$ and O$_5$ sites are superposed in a projection along the c-axis).

Fig. 2. The 24T cluster model representing the main channel of MOR framework.

represent the pore structure of MOR framework includes 24 SiO$_4$ (or AlO$_4$) tetrahedron centers (24T, Fig. 2), and contains a two-layered 12-membered main channel connected to an 8-membered side pocket. In this cluster an Al atom replaces one of the Si atoms at T$_4$ site [35,36]. To maintain the charge neutrality of the whole system, a Li$^+$ or Na$^+$ ion is incorporated near the oxygen atoms bonded to Al to produce Li- and Na-MOR, respectively. Each peripheral silicon atom in the clusters is saturated by one or two terminal hydrogen atoms. The distances between the hydrogen atoms and the corresponding silicon atoms are 1.29 Å, and the orientation of Si–H bonds is along the pre-existing Si–O bonds.

The clusters for pyridine adsorption in MOR are constructed by the partially optimized 24T model and the free optimized pyridine molecule. The pyridine molecule is placed pointing to the 12-membered ring with the nitrogen atom closing to the alkali metal ion of zeolites.

2.2. Methods

All calculations are carried out by using the ONIOM2 method in Gaussian 03 package [37]. In the two-layered ONIOM method of this work, the 6T model (shown as ball and stick in Figs. 3 and 4) of the MOR bare cluster forms the high-level layer. In the adsorption complexes, pyridine is also included in the high-level layer, while the rest of the cluster forms the low-level layer. It is known that the choice of the level of calculations for high- and low-level layers is crucial to the accuracy of the ONIOM2 methods. In this work we use the B3LYP/6-31G(d,p) density functional theory method for the high-level layer, which has been proved to be efficient in this kind of study [13–15,29]. For the low-level region, ab initio HF/3-21G and molecular mechanics force field (UFF) methods are respectively used. In ONIOM studies, hydrogen atoms are always used to link different layers to avoid chemically unrealistic model
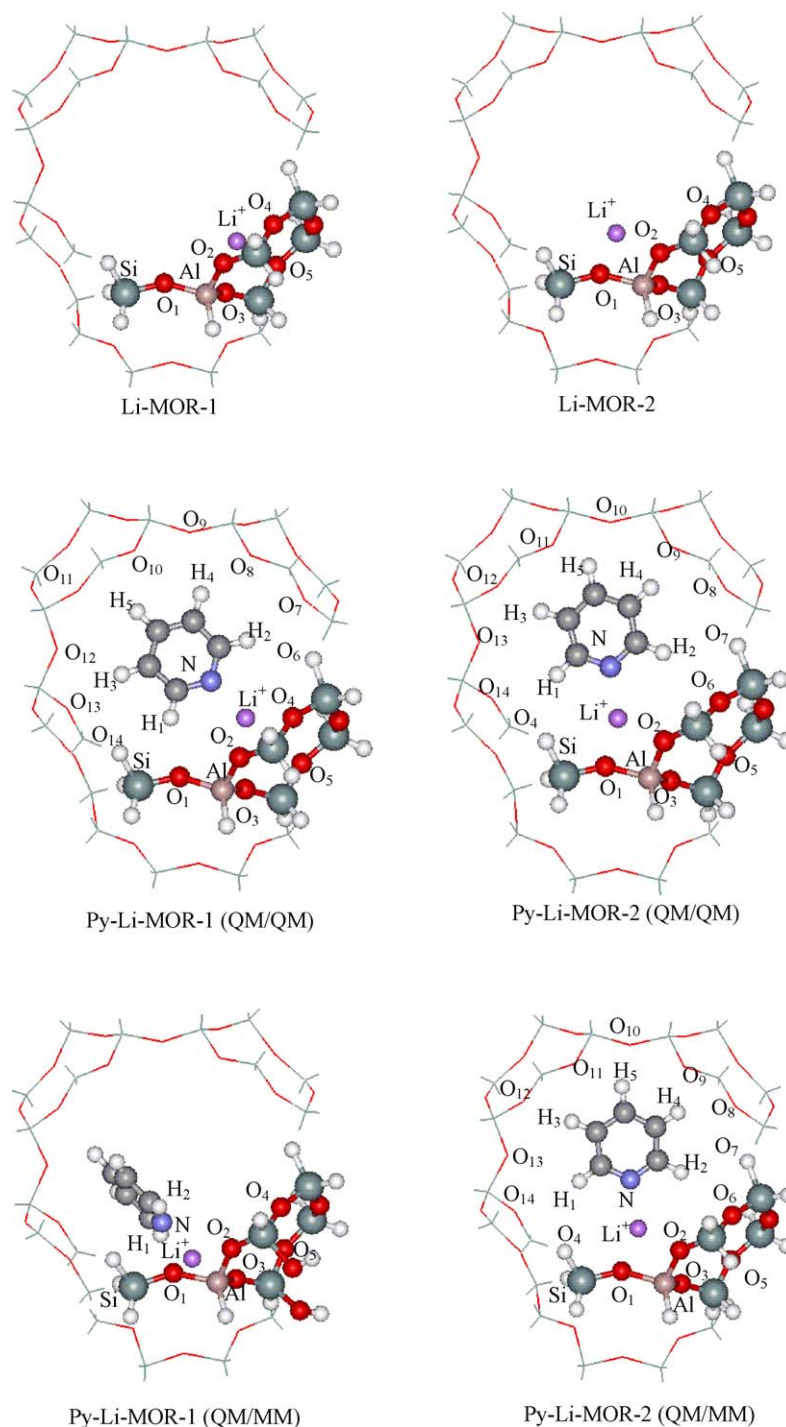
Fig. 3. The two stable Li-MOR structures and their pyridine adsorption complexes.

[13–15,25–29]. In this work, there are two possible positions to put H atoms between the high- and low-level layers. When H atoms are put between the peripheral O atoms of the 6T model and their neighboring Si atoms belonging to the low-level layer, the high-level layer is terminated by O–H groups. On the other hand, when H atoms are put between the peripheral Si atoms of 6T and their neighboring O atoms of the low-level layer, the high-level layer is terminated by Si–H groups. It was found that O–H as terminal group is not reasonable in

ONIOM2 (B3LYP/6-31G(d,p):UFF) calculations because the pyridine adsorption energies are more than two times larger than the available experimental data. In contrast, when Si–H was used, reasonable results were obtained both in ONIOM2 (QM/MM, B3LYP/6-31G(d,p):UFF) and ONIOM2 (QM/QM, B3LYP/6-31G(d,p):HF/3-21G) calculations. Therefore, the data reported here are based on models with high-level layers terminated by Si–H groups. This has been proved to be reasonable in this kind of study [14].

Na-MOR

Py-Na-MOR (QM/QM)
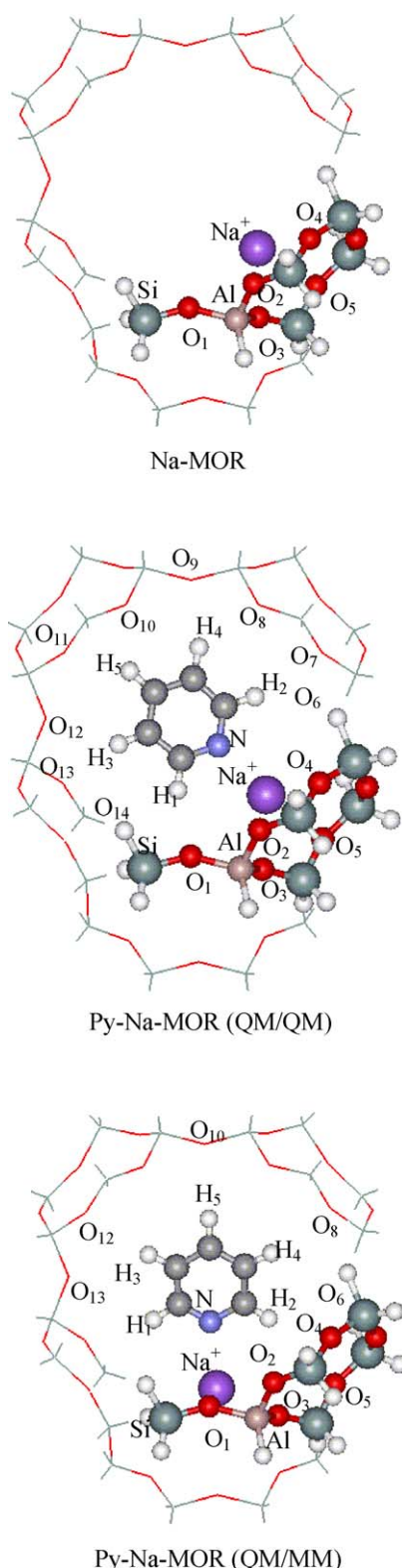

Py-Na-MOR (QM/MM)

Fig. 4. The Na-MOR cluster and its pyridine adsorption complexes.

The 24T clusters representing the structures of Li- and Na-MOR are partially optimized with the alkali ion, its neighboring Si and Al as well as the oxygen atoms surrounding Al relaxed, while the rest atoms are fixed to their crystal positions. For the adsorption complexes, the parameters of pyridine and the atoms

described above in bare MOR clusters are relaxed while the rest of the clusters are fixed.

3. Results and discussion

3.1. Structure of Li- and Na-MOR

The optimized structures of Li- and Na-MOR are presented in Figs. 3 and 4, and the structure parameters are given in Tables 1 and 2. It is found that both methods, ONIOM2 (QM/QM, B3LYP/6-31G(d,p):HF/3-21G) and (QM/MM, B3LYP/6-31G(d,p):UFF), lead to two stable structures for Li-MOR cluster (Li-MOR-1 and Li-MOR-2, Fig. 3 and

Table 1
Selected bond lengths (Å) and angles (°) of the optimized Li-MOR clusters[a]

	B3LYP/6-31G(d,p):HF/3-21G		B3LYP/6-31G(d,p):UFF	
	Li-MOR-1	Li-MOR-2	Li-MOR-1	Li-MOR-2
R_{Al-O_1}	1.753	1.787	1.728	1.776
R_{Al-O_2}	1.774	1.733	1.764	1.740
R_{Al-O_3}	1.790	1.718	1.830	1.730
R_{Si-O_1}	1.608	1.612	1.645	1.657
α_{Si-O_1-Al}	147.4	147.4	147.8	147.9
R_{Al-Li}	2.534	2.521	2.482	2.404
R_{O_1-Li}	–	1.882	–	1.917
R_{O_2-Li}	2.009	2.080	2.054	1.933
R_{O_3-Li}	2.304	–	2.118	–
R_{O_4-Li}	2.241	–	2.307	–
R_{O_5-Li}	2.727	–	2.526	–

[a] For the numbering systems, see Fig. 3.

Table 2
Selected bond lengths (Å) and angles (°) in Na-MOR cluster and its pyridine adsorption complex[a]

	B3LYP/6-31G(d,p):HF/3-21G		B3LYP/6-31G(d,p):UFF	
	Na-MOR	Py–Na-MOR	Na-MOR	Py–Na-MOR
R_{Al-O_1}	1.758	1.738	1.739	1.823
R_{Al-O_2}	1.762	1.759	1.746	1.730
R_{Al-O_3}	1.784	1.782	1.815	1.869
R_{Si-O_1}	1.608	1.601	1.646	1.671
α_{Si-O_1-Al}	147.4	147.5	147.8	147.6
R_{Al-Na}	2.778	2.830	2.689	2.732
R_{N-Na}	–	2.298	–	2.410
R_{O_1-Na}	–	–	–	2.318
R_{O_2-Na}	2.336	2.381	2.420	–
R_{O_3-Na}	2.529	2.535	2.331	2.358
R_{O_4-Na}	2.635	2.581	2.886	–
R_{O_5-Na}	2.990	2.906	2.908	–
$R_{O_1-H_1}$	–	2.266	–	–
$R_{O_6-H_2}$	–	2.990	–	2.705
$R_{O_7-H_2}$	–	2.714	–	–
$R_{O_8-H_4}$	–	2.509	–	2.909
$R_{O_9-H_4}$	–	2.307	–	–
$R_{O_{10}-H_4}$	–	2.925	–	–
$R_{O_{10}-H_5}$	–	2.528	–	2.779
$R_{O_{11}-H_5}$	–	2.551	–	–
$R_{O_{12}-H_3}$	–	2.614	–	2.938
$R_{O_{13}-H_3}$	–	2.489	–	2.742
$R_{O_{14}-H_1}$	–	2.571	–	–

[a] For the numbering systems, see Fig. 4.

Table 1). In Li-MOR-2, Li$^+$ bonds to two oxygen atoms around Al, with the Li–O distances of 1.882/2.080 and 1.917/1.933 Å, respectively. This is consistent with the symmetrical binding of Li$^+$ cation to [AlO$_4{}^-$] of other zeolite confirmed by ESR experiment [38] and other theoretical studies [39,40]. In Li-MOR-1, Li$^+$ interacts with four oxygen atoms belonging to a five-membered ring with Li–O distances ranging from 2.009 to 2.727 Å. This four-fold coordination of Li$^+$ mimics that of Na$^+$ in Na-MOR, in which Na$^+$ locates above a five-membered ring and forms four Na–O bonds 2.331–2.990 Å in length (Table 2). In a study on the Na-ZSM-5 structure [14], we found that in the intersection model of Na-ZSM-5, Na$^+$ locates above the middle of the six-membered ring and lies at short distance (2.254–2.818 Å) to four oxygen atoms and at longer distances (3.227 and 3.792 Å) to other two oxygen atoms of the ring. The location of Na$^+$ at the six-membered ring of faujasite zeolite has also been found by Vayssilov et al. [41]. In contrast, only two-fold coordination of Li$^+$ and Na$^+$ was found as stable structures for a cluster of a 20T model which did not include the eight-membered side pocket with the same ONIOM2 (QM/QM) method [29]. This indicates that the coordination of the alkali ion in zeolite pores is rather complex and depends on the pore structures, and that therefore it is sensitive to the selection of the cluster model. Obviously, the 24T model in this work is more pertinent to the MOR zeolite pore system.

The Al–Li distances in the two structures of Li-MOR are 2.534 and 2.521 Å, and the Al–Na distance in Na-MOR is 2.778 Å as calculated by the QM/QM method, which are close to 2.566 and 2.961 Å, respectively, for Al–Li and Al–Na obtained by other theoretical ONIOM study [27] and 2.506 and 2.941 Å estimated by our previous work on ZSM-5. However, the values obtained by the QM/MM method (2.482/2.404 Å for Li-MOR

and 2.689 Å for Na-MOR) are rather small. It is found that the Al–Na bond is longer than Al–Li, in agreement with the difference in radius between these two ions (Pauling radius: Li$^+$, 0.60 Å and Na$^+$, 0.95 Å [42]).

The interaction between the alkali ion and the framework oxygen atoms disturbs the Al–O and Si–O distances more or less. For instance the lattice oxygen atoms that are at short distances to Li$^+$ or Na$^+$ ion have longer bonds with Al and Si than the other oxygen atoms; i.e. Al–O$_2$ and Al–O$_3$ are longer than Al–O$_1$ in the Li-MOR-1 structure, for O$_2$ and O$_3$ are at short distances to Li$^+$. In Li-MOR-2, it is O$_1$ and O$_2$ which bond to Li$^+$, and thus Al–O$_1$ and Al–O$_2$ are longer than Al–O$_3$. Compared to the influence on bond lengths, the Si–O–Al angle is less affected by the alkali ion; it remains almost the same value in all the clusters, and is also very close to the original value of 148.0° of the initial cluster.

3.2. Structure of pyridine adsorption complexes on Li- and Na-MOR

The structures of the pyridine adsorption complexes on Li- and Na-MOR are also shown in Figs. 3 and 4, and the selected structural parameters are presented in Tables 2 and 3. It is found that there is strong electrostatic interaction between the pyridine nitrogen and the alkali metal ion with N–X distances ranging from 1.966 to 2.035 Å and 2.298 to 2.410 Å for X = Li and Na, respectively. As expected, the adsorption of pyridine in Na-MOR is weaker than that in Li-MOR, according to the weaker acidity of Na$^+$ compared to Li$^+$, which is reflected by the longer N–Na distance than N–Li. This is also reflected by the adsorption energy (see the next part). In addition to this electrostatic interaction between the zeolite and pyridine, the adsorption complexes are further stabilized by multiple hydrogen bonding between

Table 3
Selected bond lengths (Å) and angles (°) of pyridine adsorption complexes on Li-MOR clusters[a]

| | B3LYP/6-31G(d,p):HF/3-21G | | B3LYP/6-31G(d,p):UFF | |
	Py–Li-MOR-1	Py–Li-MOR-2	Py–Li-MOR-1	Py–Li-MOR-2
$R_{Al–O_1}$	1.736	1.759	1.821	1.838
$R_{Al–O_2}$	1.791	1.757	1.725	1.753
$R_{Al–O_3}$	1.753	1.728	1.874	1.790
$R_{Si–O_1}$	1.600	1.605	1.680	1.676
$R_{Al–Li}$	2.849	2.547	2.510	2.492
$\alpha_{Si–O_1–Al}$	147.4	147.4	147.6	147.6
$R_{N–Li}$	1.966	1.981	2.035	2.031
$R_{O_1–Li}$	–	1.954	1.998	1.946
$R_{O_2–Li}$	1.938	2.055	–	2.033
$R_{O_3–Li}$	–	–	1.960	–
$R_{O_4–Li}$	2.142	–	–	–
$R_{O_1–H_1(O_4–H_1)}$	2.259	(2.678)	2.762	(2.957)
$R_{O_6–H_2}$	2.722	2.859	–	2.732
$R_{O_7–H_2}$	2.699	2.993	–	2.906
$R_{O_8–H_4}$	2.410	–	–	–
$R_{O_9–H_4}$	2.428	–	–	–
$R_{O_{10}–H_5}$	2.511	2.463	–	2.649
$R_{O_{11}–H_5}$	2.645	2.687	–	2.970
$R_{O_{12}–H_3}$	2.683	2.925	–	–
$R_{O_{13}–H_3}$	2.534	2.762	–	–
$R_{O_{14}–H_1}$	2.433	2.654	–	2.915

[a] For the numbering systems, see Fig. 3.

the hydrogen atoms of pyridine and the lattice oxygen atoms of the zeolite wall with $O \cdots H$ distances ranging from 2.259 to 2.993 Å. For pyridine with rather large dimensions, the hydrogen atoms on its CH groups could reach several oxygen atoms of the zeolite wall, and thus it is difficult to have all the oxygen atoms in hydrogen bonding interaction with pyridine included in the high-level layer. This also indicates that small clusters that only include the acid site of zeolites cannot simulate this kind of interaction completely, and that the models in this work are large enough.

The coordination of pyridine nitrogen to Li^+ or Na^+ affects the Al–O and Si–O bond lengths. It has more obvious effect on the ONIOM2 (QM/MM) structures than on that of ONIOM2 (QM/QM). The Al–Li and Al–Na distances are accordingly elongated, while the Al–O–Si angle hardly changes by the adsorption. It is worth noting that in adsorption complex on Li-MOR-1, Li^+ changes the coordination from four- to two-fold to the oxygen atoms of the zeolite lattice. This indicates that in order to interact with the adsorbate more efficiently, the alkali ion has the ability to modify its position to achieve a balance between the zeolite lattice atoms and the adsorbate. For larger size Na^+ in Na-MOR, it changes the coordination to two-fold in the ONIOM2 (QM/MM) structure, while remains four-fold coordination in the ONIOM2 (QM/QM) structure, indicating that the ONIOM2 (QM/MM) method is more sensitive to the disturbance in structures than the ONIOM2 (QM/QM) method.

For comparison, pyridine adsorption on a naked Li^+ or Na^+ ion is also investigated. It is found that the formed Li–N and Na–N distances are 1.936 and 2.292 Å in Py–Li^+ and Py–Na^+ (Py, pyridine) complexes, respectively, which are shorter than those in Py–Li-MOR and Py–Na-MOR. This shows that the existence of the zeolite framework weakens the Lewis acidity of the alkali metal ions, due to the electronic and structural factors.

3.3. Pyridine adsorption energies in Li- and Na-MOR

The calculated adsorption energies on Li- and Na-MOR are given in Table 4. It can be seen that the ONIOM2 (QM/MM) method gives larger adsorption energy than the ONIOM2 (QM/QM) method. It is 195.0/192.8 and 170.6 kJ/mol for Li-MOR and Na-MOR, respectively, by the QM/MM method, and is 171.6/154.7 and 131.3 kJ/mol, respectively, by the QM/QM method. When compared to the experimental results for pyridine adsorption in Li- (153–195 kJ/mol [43]) and Na-exchanged zeolites (120 kJ/mol [43]), it can be found that the QM/MM method overestimates the adsorption energies, while the QM/QM method predicts better results.

The binding energies of pyridine on naked Li^+ and Na^+ are estimated at 208.3 and 150.1 kJ/mol. It is obvious that the energy of pyridine adsorption on Li- and Na-MOR only amounts to 82%/74% and 87% of that on bare Li^+ and Na^+, respectively, indicating the destabilizing role of the zeolite framework to the coordination of pyridine nitrogen to Li^+ or Na^+, and the weak acidity of these ions in zeolite channels. This also indicates that the dominant interaction between the pyridine probe and the alkali-exchanged zeolite is the coordination of pyridine nitrogen to the alkali metal ion. The lager adsorption energy on Li-MOR than that on Na-MOR is consistent with the lower acidity of the latter zeolite than the former.

For pyridine adsorption in Li- and Na-ZSM-5, it was found that the coordination of the nitrogen of the pyridine to the alkali cation accounts for 60% and 68% of the total adsorption energy, the rest 40% and 32% being due to the hydrogen bonds [14]. Therefore, hydrogen bonds play important roles in stabilization of the adsorption complexes.

3.4. Changes of the electronic properties upon adsorption

The selected atomic charges from Mulliken populations and calculated by the ONIOM2 (QM/QM) method on the zeolite models and their pyridine adsorption complexes are shown in Table 5. It is found that the positive charges on Li and Na decrease upon pyridine adsorption on Li-MOR-2 and Na-MOR clusters. This might be due to the electron transfer from pyridine nitrogen atom to the alkali metal ions. The charges on Li increase in the Py–Li-MOR-1 model, which resulted from two factors. In addition to the electron transfer that decreases the positive charges on Li, the changes of the coordination of Li^+ from four- to two-fold would increase the positive charge on it. This also affects the charges on Al; it increases in Py–Li-MOR-2 and Py–Na-MOR and decreases in Py–Li-MOR-1. The negative charges on the zeolite lattice oxygen atoms are also changed more or less. At the same time, the charges on the pyridine nitrogen, carbon and hydrogen atoms are all increased after adsorption, as compared to the free optimized pyridine molecule (the average charge on the hydrogen atoms is 0.097, and on the carbon and nitrogen atoms is −0.011 and −0.428, respectively), due to the polarization effect of the interaction with the zeolite lattice.

3.5. Comparison of the two methods used in this work

In this work two different ONIOM2 methods are used, i.e. the QM/QM and QM/MM methods. By comparing the optimized

Table 4
Adsorption energies (kJ/mol) of pyridine on Li- and Na-MOR cluster[a]

	B3LYP/6-31G(d,p):HF/3-21G			B3LYP/6-31G(d,p):UFF		
	E_{24T} (au)	E_{py-24T} (au)	ΔE_{ads}	E_{24T} (au)	E_{py-24T} (au)	ΔE_{ads}
Li-MOR-1	−059.22159	−9307.57954	171.6	−2154.31977	−2402.68665	195.0
Li-MOR-2	−9059.23174	−9307.58328	154.7	−2154.31980	−2402.68584	192.8
Na-MOR	−9213.99507	−9462.33769	131.3	−2309.08166	−2557.43926	170.6

[a] Energy of pyridine molecule at B3LYP/6-31G(d,p) level is −48.29260 au.

Table 5
Mulliken atomic charges on selected atoms of the bare models and their pyridine adsorption complexes in Li- and Na-MOR[a]

	Li-MOR				Na-MOR	
	Li-MOR-1	Py–Li-MOR-1	Li-MOR-2	Py–Li-MOR-2	Na-MOR	Py–Na-MOR
Al	1.498	1.487	1.528	1.535	1.470	1.488
Si	1.945	1.959	1.990	1.992	1.944	1.964
Li or Na	0.294	0.347	0.466	0.369	0.479	0.344
O_1	−1.057	−1.084	−1.083	−1.086	−1.067	−1.084
O_2	−1.056	−1.062	−1.096	−1.082	−1.086	−1.076
O_3	−1.047	−1.064	−1.065	−1.060	−1.070	−1.066
O_4	−1.116	−1.111	−1.106	−1.110	−1.119	−1.115
O_5	−1.162	−1.149	−1.143	−1.142	−1.162	−1.162
H[b]	–	0.3202	–	0.2992	–	0.3128
C[b]	–	−0.1469	–	−0.1208	–	−0.1508
N	–	−0.8119	–	−0.7942	–	−0.7853

[a] For the numbering systems, see Figs. 3 and 4.
[b] The average charge on the hydrogen or carbon atoms of pyridine.

structures of the zeolite clusters, it can be found that although there are differences in the structure parameters (bond lengths and angles) in a certain cluster, the bonding properties of the alkali metal ion in the zeolite pore are predicted to be the same by the two methods; e.g., Li$^+$ forms two- and four-fold coordination while Na$^+$ forms only four-fold coordination to the zeolite oxygen atoms. For the structures of the adsorption complexes, the two methods show some differences. QM/MM is found to be more sensitive to the adsorption of a probe molecule, reflected by the greater changes in the Al–O and Si–O bond lengths after adsorption, and by the change in the Na$^+$ coordination number in the QM/MM structure of Py–Na-MOR.

Considering the total energies for clusters, the QM/QM method shows high sensitivity to the structures. For Li-MOR, Li-MOR-2 is only slightly more stable than Li-MOR-1 by 0.05 kJ/mol in the QM/MM method, indicating the co-existence of the two structures. In the QM/QM method the energy difference between the two structures of Li-MOR is enlarged to 26.6 kJ/mol, indicating that only Li-MOR-2 in which Li$^+$ forms two-fold coordination can exist as the stable structure. This is consistent with the bonding properties of Li$^+$ in Li-ZSM-5 [14]. As for the adsorption energies in Li- and Na-MOR, the two methods show the same trends, although the QM/MM method overestimates the adsorption energies compared to the available experimental data. For instance, the adsorption energy in Li-MOR is larger than that in Na-MOR, as expected by their Lewis acidity of the two alkali ions. For getting both qualitative and quantitative results only the QM/QM method is recommended.

4. Conclusion

The structures of the Li- and Na-MOR and their interaction with pyridine were investigated by a 24T cluster model and ONIOM2 (QM/QM) as well as the (QM/MM) methods. It was found that Li$^+$ has two stable sites in Li-MOR cluster; that is two-fold or four-fold coordination to the zeolite lattice oxygen atoms. In Na-MOR Na$^+$ forms only a four-fold coordination to the lattice oxygen atoms. As compared to the calculated pyridine adsorption energies to the available experimental results, it was

found that the QM/QM method predicted better results, while the QM/MM method overestimated the adsorption energies. In addition, the energy of pyridine adsorption on Li- and Na-MOR only amounts to 82%/74% and 87% of the binding energy to naked Li$^+$ and Na$^+$ ion, respectively, indicating that the Lewis acidity of the alkali ion is weakened by interaction with the zeolite framework oxygen atoms, and that the dominant interaction between the pyridine probe and the alkali-exchanged zeolite is the coordination of pyridine nitrogen to the alkali metal ion. In addition to this kind of interaction, the adsorption complexes were further stabilized by multiple hydrogen bonds between the zeolite lattice oxygen atoms and the pyridine hydrogen atoms.

References

[1] P.E. Hathaway, M.E. Davis, J. Catal. 119 (1989) 497.
[2] A. Corma, Mater. Res. Soc. Symp. Proc. 233 (1997) 17.
[3] D. Barthomeuf, Catal. Rev. 38 (1996) 521.
[4] Z.H. Fu, Y. Ono, Catal. Lett. 21 (1993) 43.
[5] G.F. Froment, W.J.H. Dehertog, A.J. Marchi, Catalysis 9 (1992) 1.
[6] S. van Donk, A. Broersma, O.L.J. Gijzeman, J.A. van Bokhoven, J.H. Bitter, K.P. de Jong, J. Catal. 204 (2001) 272.
[7] S.P. Yuan, J.G. Wang, Y.-W. Li, H. Jiao, J. Phys. Chem. A 106 (2002) 8167.
[8] S.P. Yuan, J.G. Wang, Y.-W. Li, H. Jiao, J. Mol. Struct. (Theochem) 674 (2004) 267.
[9] P. Li, Y. Xiang, V.H. Grassian, S.C. Larsen, J. Phys. Chem. B 103 (1999) 5058.
[10] E.H. Teunissen, F.B. van Duijneveldt, R.A. van Santen, J. Phys. Chem. 96 (1992) 366.
[11] F. Haase, J. Sauer, Microporous Mesoporous Mater. 35–36 (2000) 379.
[12] H. Jobic, A. Tuel, M. Krossner, J. Sauer, J. Phys. Chem. 100 (1996) 19545.
[13] N. Jiang, S.P. Yuan, J.G. Wang, Z.F. Qin, H. Jiao, Y.-W. Li, J. Mol. Catal. A 220 (2004) 221.

[14] S.P. Yuan, W. Shi, B.R. Li, J.G. Wang, H. Jiao, Y.-W. Li, J. Phys. Chem. A 109 (2005) 2594.

[15] N. Jiang, S.P. Yuan, J.G. Wang, Z.F. Qin, H. Jiao, Y.-W. Li, J. Mol. Catal. A 232 (2005) 597.

[16] J.L. de Macedo, S.C.L. Dias, J.A. Dias, Microporous Mesoporous Mater. 72 (2004) 119.

[17] C.O. Areán, M.R.D. Delgado, G.T.P. Manoilova, A.A. Tsyganenko, E. Harrone, Chem. Phys. Lett. 262 (2002) 109.

[18] D.M. Ruthven, B.K. Kaul, Ind. Eng. Chem. Res. 32 (1993) 2047.

[19] A. Itadani, R. Kumashiro, Y. Kuroda, M. Nagao, Thermochim. Acta 416 (2004) 99.

[20] C. Paze′, S. Bordiga, C. Lamberti, M. Salvalaggio, A. Zecchina, G. Bellussi, J. Phys. Chem. B 101 (1997) 4740.

[21] K. Rozanska, Th. Demuth, F. Hutschka, J. Hafner, R.A. van Santen, J. Phys. Chem. B 106 (2002) 3248.

[22] F. Maseras, K. Morokuma, J. Comput. Chem. 16 (1995) 1170.

[23] S. Dapprich, I. Komáromi, K.S. Byun, K. Morokuma, M.J. Frisch, J. Mol. Struct. 461–462 (1999) 1.

[24] G.S. Tschumper, K. Morokuma, J. Mol. Struct. 592 (2002) 137.

[25] C. Raksakoon, J. Limtrakul, J. Mol. Struct. (Theochem) 631 (2003) 147.

[26] S. Kasuriya, S. Namuangruk, P. Treesukol, M. Tirtowidjojo, J. Limtrakul, J. Catal. 219 (2003) 320.

[27] K. Bobuatong, J. Limtrakul, Appl. Catal. A 253 (2003) 49.

[28] S. Namuangruk, P. Pantu, J. Limtrakul, J. Catal. 225 (2004) 523.

[29] N. Jiang, S.P. Yuan, J.G. Wang, Z.F. Qin, H. Jiao, Y.-W. Li, J. Mol. Catal. A 242 (2005) 105.

[30] (a) R. Buzzoni, S. Bordiga, G. Ricchiardi, C. Lamberti, A. Zecchina, Langmuir 12 (1996) 930;
(b) D. Meloni, S. Laforge, D. Martin, M. Guisnet, E. Rombi, V. Solinas, Appl. Catal. A 215 (2001) 55.

[31] H.G. Karge, V. Dondur, J. Weitkamp, J. Phys. Chem. 95 (1991) 283.

[32] G. Defosse, P. Canesson, J. Chem. Soc., Faraday Trans. I 72 (1976) 2265.

[33] J.A. Ripmeester, J. Am. Chem. Soc. 105 (1983) 2925.

[34] M.M.J. Treacy, J.B. Higgins, R. von Ballmoos, Zeolites 16 (1996) 751.

[35] E.G. Derouane, J.G. Fripiat, Proceedings of the Sixth International Zeolite Conference, Reno, July 1983, p. 717.

[36] S.P. Yuan, J.G. Wang, Y.-W. Li, S.Y. Peng, J. Mol. Catal. A 175 (2001) 131.

[37] Gaussian 03, Revision B.04, Gaussian, Inc., Pittsburgh, PA, 2003.

[38] H. Hosono, H. Kawazoe, J. Nishii, J. Kanazawa, J. Non-Cryst. Solid 51 (1982) 217.

[39] K. Bobuatong, J. Limtrakul, J. Appl. Catal. A 253 (2003) 49.

[40] R.C. Deka, R.K. Roy, K. Hirao, Chem. Phys. Lett. 332 (2000) 576.

[41] G.N. Vayssilov, M. Staufer, T. Belling, K.M. Neyman, H. Knözinger, N. Rösch, J. Phys. Chem. B 103 (1999) 7920.

[42] From the world wide web http://www.webelements.com.

[43] H. Bludau, H.G. Karge, W. Niessen, Microporous Mesoporous Mater. 22 (1998) 297.